



Harnessing Cucurbitaceae Seed Extracts for Natural Suppression of Uric Acid and Calcium Urate Crystallization: An Invitro Biocrystallization Analysis

R Selvaraju^{1*} and S.D. Ravi Sharma^{2*}

^{1,2}Department of Physics, Annamalai University, Annamalai Nagar, Tamil Nadu, India.

(Received: 28 January 2026 Revised: 16 March 2026 Accepted: 09 April 2026)

KEYWORDS

Uric acid,
Calcium urate,
Biocrystallization,
Momordica charantia,
Cucumis sativus,
Cucurbita pepo,

ABSTRACT:

Background: Uric acid (UA) and Calcium Urate (CaU) crystals are important biominerals associated with gout, urolithiasis and nephropathy related to hyperuricemia. Despite their clinical significance, plant based strategies for inhibiting these crystals are still underexplored, particularly with regard to extracts from Cucurbitaceae seeds.

Method: This present study investigates the invitro growth and inhibition of UA and CaU crystals using aqueous seed extracts from three Cucurbitaceae species: *Cucumis sativus* (Cucumber), *Cucurbita pepo* (Pumpkin) and *Momordica charantia* (bitter gourd). Phytochemical screening was performed to characterize the secondary metabolite profiles of all three extracts. For the inhibition study, the crystals were grown using the single diffusion silica gel growth method. The extracts were prepared at various concentrations of 0%, 25%, 50%, 75% and 100%. The crystals were harvested after a period of 21 days. The length of the crystals were measured using ImageJ software, while the mass was recorded gravimetrically.

Results: All extracts were found to be rich in flavonoids, saponins, phenolics, tannins and terpenoids. For uric acid crystals, *M. Charantia* exhibited the greatest reduction in length (80%) and mass (79.4%) at 100% concentration, while *C. sativus* also achieve an 80% reduction in length. *M. Charantia* showed a length reduction of 71.43% and a mass reduction of 86.4% marking the highest results among all tested extracts.

Conclusions: Extracts from Cucurbitaceae seeds especially from *Momordica charantia* demonstrate significant anticrystallization activity depend on the concentration, likely due to their rich phytochemical content. These findings support the ethnopharmacological relevance of these seeds in managing urate related disorders and suggest their potential as promising for further pharmacological development.

1. Introduction

Uric acid (2,6,8-trioxypurine) is the final product of purine metabolism in humans. It is formed through the sequential oxidation of hypoxanthine and xanthine, catalysed by the enzyme xanthine oxidase. When serum urate concentrations exceed the physiological solubility threshold of approximately 6.8mg/dL, urate salts can crystallize in joints and kidneys, leading to conditions such as gout, kidney stones (urolithiasis) and tubulointerstitial nephropathy [1-4]. The deposition of urate crystals, particularly in articular cartilage, synovial fluid and renal tubular epithelium, poses a significant global health burden, with the prevalence of gout exceeding 3-4% in many populations [2,3].

Among various forms of urate crystals, calcium urate (CaU) is increasingly recognized as a significant contributor to the formation of mixed urinary stones [1]. Its compact, nodular

crystal structure and its ability to promote the secondary nucleation of calcium urate through epitaxial interactions make it particularly relevant for dissolution and inhibition strategies. Despite its clinical significance, calcium urate has attracted considerably less research attention than the monosodium urate and calcium oxalate [5,7].

Currently, the pharmacological management of hyperuricemia and gout primarily relies on xanthine oxidase inhibitors (such as allopurinol and febuxostat) and uricosuric agents (like probenecid and benzbromarone) [5,6]. However, these medications can have significant adverse effects, including hepatotoxicity, hypersensitivity reactions and possible drug interactions. These side effects limit their long-term use and present genuine clinical challenges. As a result, there is renewed interest in exploring plant-derived inhibitors of urate crystallization as safer, alternative treatments [6].



Ethnopharmacological records from Ayurvedic, Unani and Siddha medical traditions document various *Cucurbita* preparations used in treating renal and metabolic disorders, including urolithiasis and conditions resembling hyperuricemia [8]. Seed of *Cucumis sativus* (cucumber)[9,10], *Cucurbita pepo* (pumpkin) [11] and *Momordica charantia* (bitter melon) [12,16,17,18,19] are rich in flavonoids (such as Quercetin, kaempferol and luteolin derivatives), cucurbitacins, phytosterols, saponins and phenolic acids (including caffeic, ferulic and gallic acids) as well as bitter cucurbitane-type triterpenoids. These secondary metabolites have documented properties that inhibit xanthine oxidase, chelate polyvalent cations and disrupt crystal growth through selective adsorption mechanisms [11-15].

In vitro crystal growth studies using the single diffusion silica gel method provide a reliable, reproducible model for investigating the nucleation and growth kinetics of pathological crystals under conditions that mimic physiological supersaturation [4,20,23,24]. This technique allows for the systematic evaluation of varying inhibitor concentrations affecting crystal morphology, size and mass outcomes that are directly relevant to the potential clinical application of a therapeutic agent.

This study presents the first comprehensive comparative in vitro investigation of the inhibitory effect of aqueous seed extracts from *Cucumis sativus*, *Cucurbita pepo* and *Momordica charantia* on the growth of uric acid and calcium urate crystals. The crystal morphology, length reduction and mass reduction across five various concentrations are analysed. Phytochemical profiling provides a mechanistic context for the observed inhibitory activities and supports the rationale for developing these seed extracts as anti-urolithic agents.

2. Materials and Methods

2.1 Plant material collection and authentication

Seeds of *Cucumis sativus* L. (cucumber), *Cucurbita pepo* L. (pumpkin) and *Momordica charantia* L. (Bitter melon) were obtained from a Vegetable Research Centre in Palur, Tamil Nadu, India. A qualified botanist conducted taxonomic authentication before beginning the experimental procedures. The collected seeds were washed under running tap water, followed by rinsing with distilled water to remove surface contaminants. The samples were then air-dried in a well-ventilated area, shielded from direct sunlight and subsequently over-dried at 40-50°C until a constant mass was achieved. This step ensured complete moisture removal while preserving thermolabile bioactive constituents.

2.2 Preparation of seed Powder and aqueous extract

The dried seed material was mechanically pulverized using an electric grinder and further ground with a mortar and pestle to create a fine, homogenous powder. The powder was then passed through standard mesh sieves to ensure uniform particle size distribution. Aqueous extracts were prepared at a 1:20 (w/v) solid to solvent ratio using double-distilled water. The mixture was stirred on a magnetic stirrer for 1 hour and concentrated by gentle heating to achieve a final volume of 100mL per batch. Filtered extracts were stored at 4°C. Fresh working dilutions of 0%, 25, 50%,75% and 100% (v/v in distilled water) were prepared before each crystallization experiment to prevent degradation of bioactive constituents.

2.3 Phytochemical screening

Qualitative phytochemical analyses were conducted on all three seed extracts using standard colorimetric and precipitation reactions to detect the following: flavonoids (alkaline reagent test), phenolic compounds (ferric chloride test), tannins (lead acetate test), saponins (froth test), terpenoids/triterpenoids (Salkowski test), steroids/phytosterols (Liebermann–Burchard test), glycosides (Keller–Killiani test), alkaloids (Dragendorff reagent), carbohydrates (Molisch test), and lipids/fixed oils (Sudan III test). The relative abundance of each phytochemical was scored as high (+++), moderate (++), or low/trace (+) [31-36].

2.4 Crystal growth by single diffusion silica gel method

Crystallization was performed in borosilicate glass tubes (200 mm in length and 20 mm in internal diameter). Silica gel was prepared by titrating 0.5 M sodium metasilicate (SMS) solution with glacial acetic acid (99.8%) under constant stirring at room temperature until a final pH of 5.0 was reached. The gel density was adjusted to 1.04 g/cm³ by controlling the concentration of SMS. The gels were allowed to set undisturbed for 48 hours at ambient temperature.

2.4.1 Uric acid (UA) crystal system

A 0.5 M uric acid solution was created by dissolving uric acid powder in 20 mL of 0.2 M NaOH with gentle heating and stirring for 1 hour. This solution, combined with the appropriate concentration (0%, 25%, 50%, 75% and 100%) of seed extract, was carefully layered onto the set gel. Crystals were allowed to grow for 21 days at room temperature.

2.4.2 Calcium urate (CaU) crystal system

Uric acid was dissolved in 0.2 M NaOH, as described above, to form a sodium urate intermediate. A 0.3 M CaCl₂ solution was added dropwise with continuous stirring over a period of 3 hours to ensure complete ionic exchange and equilibration. The pH was adjusted to 7.0 using glacial acetic



acid, and the final volume was set to 20 mL. This solution, combined with seed extract at each test concentration, was then layered onto the gel. The growth period was 21 days. All experiments were conducted in triplicate, with untreated controls (0% extract) crystal system.

2.5 Crystal characterization

After 21 days, harvested crystals were photographed under consistent lighting conditions. The harvested crystals length were measured using ImageJ software (NIH, USA), with scale bars in the photographs serving as calibration references. For each experimental condition, the average, maximum and minimum crystal lengths were recorded from a minimum of five crystals. Crystal mass was determined using a digital analytical balance with a precision of ± 0.001 g. Inhibitory efficacy was quantified as follows:

$$\text{Reduction (\%)} = \frac{\text{Control value} - \text{Treated value}}{\text{Control value}} \times 100 \quad (1)$$

3. Results and Discussion

3.1 Phytochemical composition of seed extracts

Qualitative phytochemical screening revealed a diverse and complementary profile of secondary metabolites across all three seed extracts (Table 1). All three species tested positive for all ten phytochemical classes, although there were quantitative differences in their relative abundances. *Momordica charantia* L. and *Cucurbita pepo* L. seeds exhibited a high abundance (+++) of flavonoids and phenolic compounds, while *M. charantia* also showed a high content of saponins. Notably, *Cucurbita pepo* L. was distinguished by its exceptionally high levels of phytosterols and lipid/fixed oil. These profiles provide a mechanistic basis for the observed inhibitory activities on crystal formation. Flavonoids and cucurbitacin act through xanthine oxidase inhibition and crystal face adsorption, phenolic acids and tannins function through Ca^{2+} chelation and urate solubilization, and saponins disrupt crystal lattice surfaces through their amphiphilic properties [25-30]

Table 1. Phytochemical screening of Cucurbitaceae seed extracts

Phytochemical	<i>C. sativus</i>	<i>C. pepo</i>	<i>M. charantia</i>
Flavonoids	+++	+++	+++
Phenolic compounds	++	+++	+++
Tannins	++	++	++
Saponins	++	++	+++
Terpenoids/Triterpenoids	++	++	++

Steroids/Phytosterols	++	+++	++
Glycosides	+	++	++
Alkaloids	+	++	++
Carbohydrates	++	++	++
Lipids/Fixed Oils	++	+++	++

(+++ High, ++ Moderate, + Low/trace presence)

3.2 Uric acid crystal inhibition

3.2.1 Morphology of Uric acid crystals under the influence of the extracts

All three seed extracts such as *Cucumis sativus*, *Cucurbita pepo* and *Momordica charantia* showed similar uric acid crystal morphologies at 0% UA concentration, with large, flat, elongated structures shown in Fig.1 (a,b)-3 (a,b). As concentrations increased, crystals fragmented: at 25% UACS, they turned into smaller, irregular fragments; at 50% UACS, they became rough, nodular pieces; and at 75% UACS, the crystals were jagged and granular. By 100% UACS, fine, crumbled crystals dominated. *Cucurbita pepo* exhibited marginally less aggressive disruption at 25% UACP concentration compared to *Cucumis sativus*, resulting in larger irregular fragments. At 75% UACP, *Cucurbita pepo* produced fine, rounded granules, indicating smoother disruption of crystal growth. *Momordica charantia* was notably effective; at 25% UAMC, its crystals were irregularly fragmented, comparable in size to the other extracts. At 50% UAMC, the crystals showed moderate fragmentation. However, at 75%UAMC, it produced a mix of flat and granular forms, suggesting different inhibition kinetics. At 100% UAMC, it yielded the most fragmented population of fine, irregular particles.

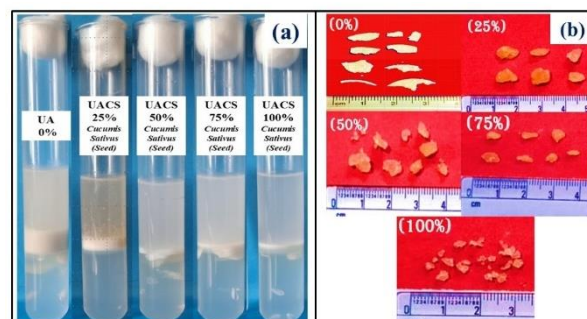


Fig. 1(a) Uric acid crystals grown in single gel diffusion method under the influence of *Cucumis sativus* (seed) extract, 1(b) Harvested uric acid crystals in different concentrations of 0%, 25%, 50%, 75% and 100% by *Cucumis sativus* (Seed)

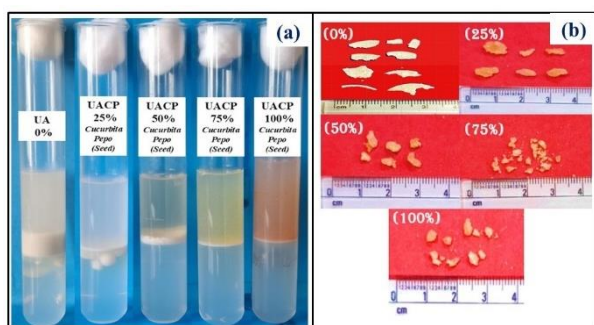


Fig. 2(a)Uric acid crystals grown in single gel diffusion method under the influence of Cucurbita pepo (seed) extract, 2(b) Harvested uric acid crystals in different concentrations of 0%, 25%, 50%, 75% and 100% by Cucumis sativus (Seed)

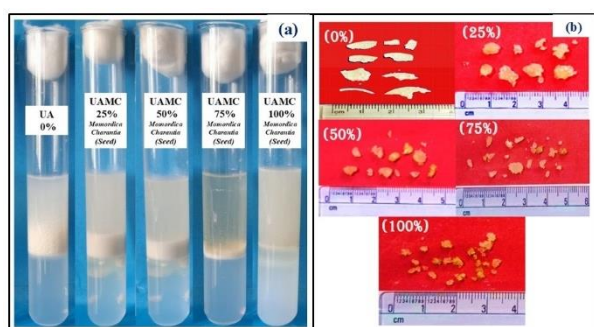


Fig. 3(a)Uric acid crystals grown in single gel diffusion method under the influence of Momordica charantia (seed) extract, 3(b) Harvested uric acid crystals in different concentrations of 0%, 25%, 50%, 75% and 100% by Cucumis sativus (Seed)

Table.1a Length of the harvest uric acid crystal under the influence of Cucumis sativus (seed), Cucurbita pepo (seed) and Momordica charantia (seed) extracts at various concentration of (0%, 25%, 50%,75% and 100%)

Concentration %	Length of the crystal (cm)								
	Cucumis sativus (Seed)			Cucurbita pepo (Seed)			Momordica charantia (Seed)		
	Average	Maximum	Minimum	Average	Maximum	Minimum	Average	Maximum	Minimum
0%	1.5	2.1	0.9	1.5	2.1	0.9	1.5	2.1	0.9
25%	0.7	0.9	0.5	0.9	0.9	0.5	0.6	0.8	0.4
50%	0.55	0.8	0.3	0.7	0.7	0.3	0.45	0.6	0.3
75%	0.45	0.6	0.3	0.6	0.6	0.2	0.4	0.6	0.2
100%	0.3	0.5	0.1	0.4	0.4	0.1	0.3	0.5	0.1

Table. 1b Reduction% of average length of the uric acid crystal under the influence of Cucumis sativus (seed), Cucurbita pepo (seed) and Momordica charantia (seed) extract

Concentration	Cucumis sativus UACS		Cucurbita pepo UACP		Momordica charantia UAMC	
	Average length (cm)	Reduction % (from 0%)	Average length (cm)	Reduction % (from 0%)	Average length (cm)	Reduction % (from 0%)
0%	1.5	—	1.5	—	1.5	—
25%	0.7	53.33%	0.9	40%	0.6	60%
50%	0.55	63.33%	0.7	53.33%	0.45	70%
75%	0.45	70%	0.6	60%	0.4	73.33%
100%	0.3	80%	0.4	73.33%	0.3	80%

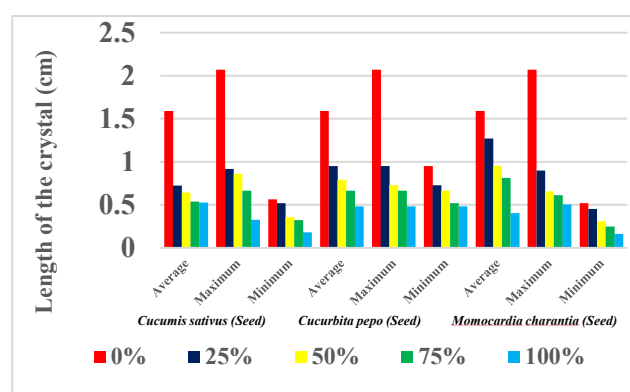


Fig. 4 Bar diagram of length of the harvest uric acid crystal under the influence of Cucumis sativus (seed), Cucurbita pepo (seed) and Momordica charantia (seed) extracts at various concentration of (0%, 25%, 50%,75% and 100%)

3.2.2 Length of Uric acid crystals under the influence of the extracts

Crystals were measured using ImageJ after a 21-day inhibition period across five concentrations (0%, 25%, 50%, 75%, and 100%). Table.1a shows the Length of the harvest uric acid crystal under the influence of Cucumis sativus (seed), Cucurbita pepo (seed) and Momordica charantia (seed) extracts at various concentration of (0%, 25%, 50%,75% and 100%), Table. 1b gives the Reduction% of average length of the uric acid crystal under the influence of Cucumis sativus (seed), Cucurbita pepo (seed) and Momordica charantia (seed) extract. and Fig. 4 shows the Bar diagram of length of the harvest uric acid crystal under the influence of Cucumis sativus (seed), Cucurbita pepo (seed) and Momordica charantia (seed) extracts at various concentration of (0%, 25%, 50%,75% and 100%)



All extracts had an average length of 1.5 cm at 0% concentration. *Cucumis sativus* demonstrated rapid inhibition, reducing crystal length to 0.2 cm (80% reduction) at 100% UACS. The most significant drop (53.33%) occurred at 25% UACS, indicating its high potency as a crystal inhibitor. At 50% UACS, the average length was 0.55 cm, showing a cumulative reduction (63.33%) effect as concentration increased. At the 75% UACS, the average length was reduced to 0.45cm, with the cumulative reduction 70%, and the average length was reduced to 0.3cm with the overall cumulative reduction of 80% under 100% of UACS extract.

For *Cucurbita pepo* at 25% UACP concentration, crystal length decreased to 0.9 cm, a 40% reduction from the control, representing the largest single decrement (0.6 cm) from control. This indicates strong inhibitory effects on crystal growth even at low doses, suggesting the presence of bioactive compounds. At 50% UACP concentration, crystal length declined further to 0.7 cm, achieving a cumulative reduction of 53.33% and at the 75% UACP, the average length was reduced to 0.6cm, with the cumulative reduction 60% and at 100% UACP, it reached 0.4 cm, with maximum cumulative inhibition of 73.33%. The extract's inhibitory capacity appears to approach a saturation point, especially noted from 75% UACP to 100% UACP, where a 0.2 cm drop indicates a recovery in effect.

For *Momordica charantia* at 25% UAMC, crystal length dropped to 0.6 cm, achieving a 60% reduction—the most significant at this concentration across all extracts. This highlights its rapid action, surpassing other extracts even at lower concentrations. At 50% UAMC, the length decreased to 0.45 cm (70% inhibition), and at 75% UAMC, it reached 0.4 cm (73.33% inhibition). The smallest decrement was noted at this stage, indicating near saturation of inhibitory mechanisms. Finally, at 100% UAMC, crystal length reached 0.3 cm, reflecting an 80% cumulative inhibition and a strong performance comparable to *Cucumis sativus*.

Table.2 Cross-extract comparison

Parameter	<i>Cucumis sativus</i> (Seed)	<i>Cucurbita pepo</i> (Seed)	<i>Momordica charantia</i> (Seed)
Average length (25%)	0.7cm	0.9cm	0.6cm
Final average length (100%)	0.3cm	0.4cm	0.3cm
Maximum Reduction %	80%	73.33%	80%

Overall, from 0% UAMC to 25% UAMC, the most powerful first-step inhibition was recorded with *M. charantia*, exceeding other extracts. The data highlights the rapid

engagement of bioactive molecules in *M. Charantia* inhibiting uric acid crystallization. The table.2 shows the cross extract comparison of uric acid crystal. From Maximum reduction% it confirms that the *Cucumis sativus* and *Momordica charantia* (seed) extract exhibit higher percentage of length reduction on uric acid crystal when compared to *Cucurbita pepo* (seed) extract.

3.2.3 Mass of Uric acid crystals under the influence of the extracts

Table. 3a Mass of the harvested uric acid crystal under the influence of *Cucumis sativus* (seed), *Cucurbita pepo* (seed) and *Momordica charantia* (seed) extracts at various concentrations (0%, 25%, 50%,75% and 100%)

Concentration of the Extract	Name of the Extract / Mass of the Crystal (g)		
	<i>Cucumis sativus</i> (seed)	<i>Cucurbita pepo</i> (seed)	<i>Momordica charantia</i> (seed)
0%	0.68	0.68	0.68
25%	0.36	0.55	0.44
50%	0.32	0.39	0.31
75%	0.27	0.32	0.25
100%	0.24	0.25	0.14

Table. 3b Reduction% of average length of the uric acid crystal under the influence of *Cucumis sativus* (seed), *Cucurbita pepo* (seed) and *Momordica charantia* (seed) extract

Concentration	<i>Cucumis sativus</i> (seed)-UACS		<i>Cucurbita pepo</i> (seed)-UACP		<i>Momordica charantia</i> (Seed) - UAMC	
	Mass (g)	Reduction (%)	Mass (g)	Reduction (%)	Mass (g)	Reduction %
0% ↓ 25%	0.68 ↓ 0.36	0.32g (47.1%)	0.68 ↓ 0.55	0.13g (19.1%)	0.68 ↓ 0.44	0.24g (35.3%)
25% ↓ 50%	0.36 ↓ 0.32	0.04g (11.1%)	0.55 ↓ 0.39	0.16g (29.1%)	0.44 ↓ 0.31	0.13g (29.5%)
50% ↓ 75%	0.32 ↓ 0.27	0.05g (15.6%)	0.39 ↓ 0.32	0.07g (17.9%)	0.31 ↓ 0.25	0.06g (19.4%)
75% ↓ 100%	0.27 ↓ 0.24	0.0g (11.1%)	0.32 ↓ 0.25	0.07g (21.9%)	0.25 ↓ 0.14	0.11g (44.0%)

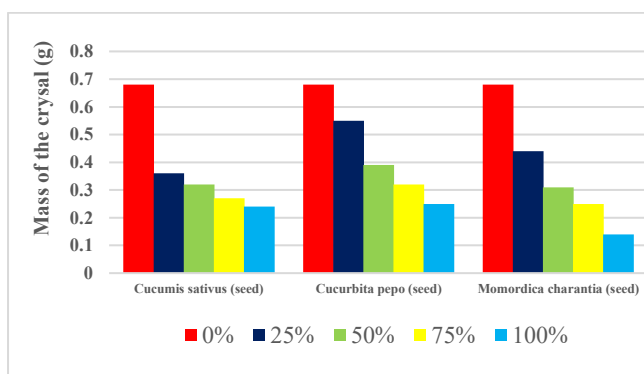


Fig.5 Bar diagram of the mass of the harvest uric acid crystal under the influence of *Cucumis sativus* (seed), *Cucurbita pepo* (seed) and *Momordica charantia* (seed) extracts at various concentration of (0%, 25%, 50%,75% and 100%)

All the plant seed extracts, *cucumis sativus*, *cucurbita pepo* and *momordica charantia* demonstrated measurable uric acid crystal dissolution activity across an ascending concentration gradient of (0-100%), with a uniform baseline crystal mass of 0.68g serving as the untreated control. Table. 3a shows the mass of the harvested uric acid crystal under the influence of *Cucumis sativus* (seed), *Cucurbita pepo* (seed) and *Momordica charantia* (seed) extracts at various concentrations (0%, 25%, 50%,75% and 100%), Table. 3b gives the Reduction% of average length of the uric acid crystal under the influence of *Cucumis sativus* (seed), *Cucurbita pepo* (seed) and *Momordica charantia* (seed) extract and Fig.5 shows the Bar diagram of length of the harvest uric acid crystal under the influence of *Cucumis sativus* (seed), *Cucurbita pepo* (seed) and *Momordica charantia* (seed) extracts at various concentration of (0%, 25%, 50%,75% and 100%). However, the extracts differed markedly in their dissolution kinetics, concentration response profiles and cumulative efficacy.

Cucumis sativus (cucumber) seed extract exhibited the most precipitous initial reduction, with the crystal mass declining sharply from 0.68g to 0.36g at the lowest concentration tested (25% UACS), corresponding to 47.1% reduction. This disproportionately large early-stage response implies the presence of highly reactive, low-threshold bioactive constituents, likely cucurbitacin, flavonoids, and tannins, capable of initiating crystal solubilization at dilute concentrations. Activity subsequently through mid-range (25-75%) with incremental reductions of approximately 11.1-15.6% per step, before modest further dissolution at full concentration. The cumulative reduction of 0.44g (64.7%) from the control reflects strong front-loaded uricolytic performance.

Cucurbita pepo (Pumpkin) seed extract demonstrated a distinctly different, more graduate dissolution profile. The initial reduction of 25% UACP concentration was comparatively modest (0.13g: 19.1%), suggesting that its bioactive constituents, putatively phytosterols, saponins and phenolic compounds require higher concentration thresholds to achieve effective uric acid solubilization. Peak activity occurred in the mid-range (25-50%) where the largest single step reduction of 0.16g (29.1%) was recorded, followed by uniform decrements of 0.07g at both the 50-75% and 75-100% intervals. This biphasic pattern, characterized by mid-range acceleration and sustained upper range activity is consistent with a multicomponent mechanism in which distinct phytochemical fractions exert activity at different concentration. The final cumulative reduction of 0.30g (63.2%) was comparable to *Cucumis sativus*, though achieved through a more evenly distributed dissolution trajectory.

Momordica charantia (bitter gourd) seed extract demonstrated the greatest overall uricolytic efficacy among the three species evaluated, achieving a total crystal mass reduction of 0.54 g (79.4%) the highest cumulative dissolution. At 25% UAMC concentration (0.24g: 35.3%) attributable to the well documented phytochemical richness of bitter gourd seeds including Momordica, charantia, alkaloids and flavonoids with established anti-hyperuricemia properties; and a remarkable terminal surge at the 75-100% concentration step, where the single largest percentage reduction across all extracts (0.11g; 44%). This late stage potentiation suggests the involvement of sparingly soluble bioactive fractions that only reach effective concentrations at maximum extract strength, a mechanistic inference consistent with the known complexity of *Momordica charantia* phytochemical composition. The final residual crystal mass of 0.14g at 100% concentration. All three seed extracts possess uricolytic potential; *Momordica charantia* is more efficient in reducing the mass of the crystal due to this unique concentration-dependent kinetics.

Table. 4 Cumulative mass reduction % across all the extracts

Seed Extract	Final Mass (g)	Total Mass Reduced (g)	% Total Reduction
<i>Cucumis sativus</i>	0.24	0.44	64.7%
<i>Cucurbita pepo</i>	0.25	0.43	63.2%
<i>Momordica charantia</i>	0.14	0.54	79.4%



From Mass reduction%, it confirms that the *Momordica charantia* (seed) extract exhibits a higher percentage of mass reduction of 79.4% on uric acid crystal when compared to *Cucumis sativus* and *Cucurbita pepo* (seed) extract. Table.4 provides a cumulative mass reduction % across all the extract From the length and mass reduction %, *Momordica charantia* exhibit higher reduction % of 80% of length and 79.4% of mass.

3.3 Calcium urate inhibition

3.3.1 Morphology of calcium urate crystals under the influence of the extracts

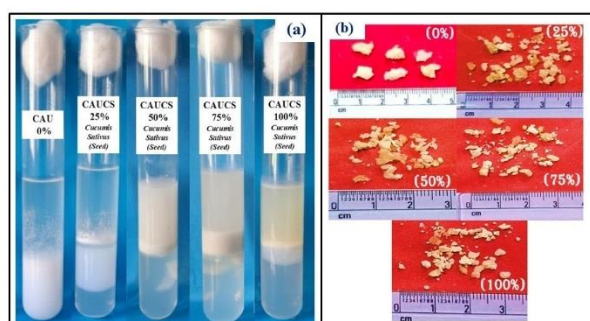


Fig. 6(a) Calcium urate crystals grown in single gel diffusion method under the influence of *Cucumis sativus* (seed) extract, **6(b)** Harvested Calcium urate crystals in different concentrations of 0%, 25%, 50%, 75% and 100% by *Cucumis sativus* (Seed)

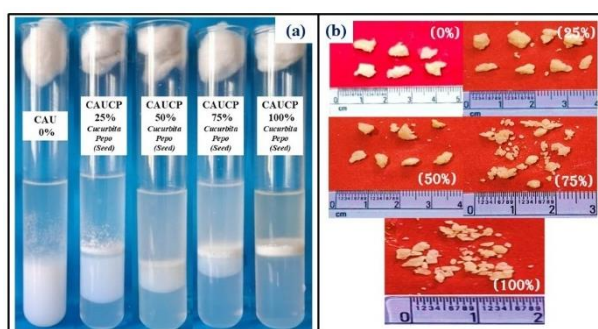


Fig. 7(a) Calcium urate crystals grown in single gel diffusion method under the influence of *Cucurbita pepo* (seed) extract, **7(b)** Harvested Calcium urate crystals in different concentrations of 0%, 25%, 50%, 75% and 100% by *Cucurbita pepo* (Seed)

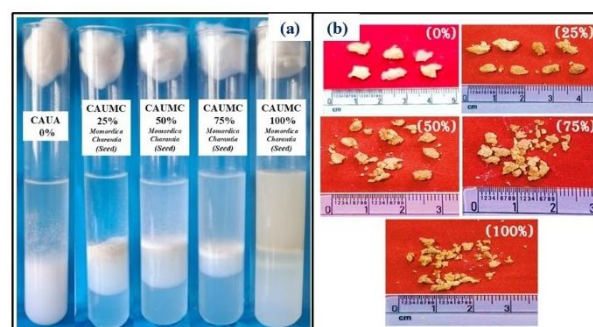


Fig. 8(a) Calcium urate crystals grown in single gel diffusion method under the influence of *Momordica charantia* (seed) extract, **8(b)** Harvested Calcium urate crystals in different concentrations of 0%, 25%, 50%, 75% and 100% by *Momordica charantia* (Seed)

The calcium urate crystals harvested at a 0% concentration showed compact, nodular shapes that differed from the UA controls. With *Cucumis sativus* seed extract, a complex pattern of inhibition emerged. Fig. 6(a,b)- 8(a,b) shows Calcium urate crystals grown in a single gel diffusion method under the influence of (seed) extract and Harvested Calcium urate crystals in different concentrations of 0%, 25%, 50%, 75% and 100% by *Momordica charantia* (Seed)

At 25% concentration, crystal fragments increased in number but decreased in size, displaying rougher edges. The extract enhanced crystal nucleation while limiting crystal size. At 50%, the fragmentation intensified, showing smaller, irregular flakes. By 75%, the crystals were even smaller and more uniform, indicating further inhibition of growth. At 100%, the extract produced the finest, most widely distributed fragments, reflecting maximum inhibitory effects. In contrast, the morphology of calcium urate crystals influenced by *Cucurbita pepo* (pumpkin) seed extract maintained a nodular form at intermediate concentrations. At 25%, the fragments were smaller and more spaced, suggesting disruption of aggregation. By 50%, pieces became irregular and flakier. At 75%, the crystals were more numerous and chip-like, indicating significant disruption. At 100%, the extract led to finely fragmented granules densely packed on the collection surface, illustrating surface erosion effects. *Momordica charantia* seed extract demonstrated the most distinctive crystal pattern. At 25%, crystals were smaller but retained a chunky morphology. At 50%, there was a significant increase in fragments with rough, etched surfaces. By 75%, fragments were finer and more numerous, and at 100%, the extract produced the most fragmented debris, exhibiting a pronounced rough texture among all extracts tested.



3.3.2 Length of calcium urate crystals under the influence of the extracts

Table .5(a) Length of the harvest Calcium urate crystal under the influence of *Cucumis sativus* (seed), *Cucurbita pepo* (seed) and *Momordica charantia* (seed) extracts at various concentrations (0%, 25%, 50%,75% and 100%)

Concentration %	Length of the crystals (cm)								
	<i>Cucumis sativus</i> (Seed)			<i>Cucurbita pepo</i> (Seed)			<i>Momordica Charantia</i> (Seed)		
	Average	Maximum	Minimum	Average	Maximum	Minimum	Average	Maximum	Minimum
0%	1.05	1.5	0.6	1.05	1.5	0.6	1.05	1.5	0.6
25%	0.9	1.3	0.5	0.8	1	0.6	0.6	0.8	0.4
50%	0.8	1.2	0.4	0.7	0.9	0.5	0.55	0.8	0.3
75%	0.75	1	0.5	0.5	0.8	0.2	0.45	0.7	0.2
100%	0.5	0.8	0.2	0.4	0.7	0.1	0.3	0.4	0.2

Table. 5(b)Reduction% of average length of the Calcium urate crystal under the influence of *Cucumis sativus* (seed), *Cucurbita pepo* (seed) and *Momordica charantia* (seed) extract

At 0% concentration, all three seed extracts had an average calcium urate crystal length of 1.05cm. Increasing the concentration from 0% to 100% resulted in a dose-dependent reduction in average crystal length across the extracts, each demonstrating different levels of inhibition. Table .5a represents the Length of the harvest Calcium urate crystal under the influence of *Cucumis sativus* (seed), *Cucurbita pepo* (seed) and *Momordica charantia* (seed) extracts at various concentration of (0%, 25%, 50%,75% and 100%),Table.5b Reduction% of average length of the Calcium urate crystal under the influence of *Cucumis sativus* (seed), *Cucurbita pepo* (seed) and *Momordica charantia* (seed) extract and Fig. 9 displays the Bar diagram of length of the harvest calcium urate crystal under the influence of *Cucumis sativus* (seed), *Cucurbita pepo* (seed) and *Momordica charantia* (seed) extracts at various concentration of (0%, 25%, 50%,75% and 100%)

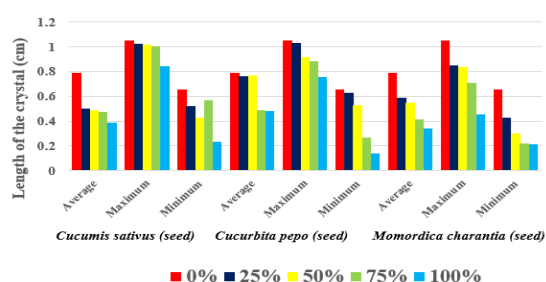


Fig.9 Bar diagram of length of the harvest calcium urate crystal under the influence of *Cucumis sativus* (seed),

Cucurbita pepo (seed) and *Momordica charantia* (seed) extracts at various concentration of (0%, 25%, 50%,75% and 100%)

Cucumis sativus showed gradual decreases in average crystal length, starting at 1.05cm and dropping to 0.9cm at 25% concentration (14.3% reduction), and continuing to 0.5cm at 100% (33.3% reduction). The total reduction was 0.55cm (52.4%), with maximum lengths decreasing from 1.5cm to 0.8cm. *Cucurbita pepo* responded more significantly, dropping to 0.8cm at 25% (23.8% reduction) and reaching 0.4cm at 100% (20% reduction), totaling 0.65cm (61.9%). Notably, its minimum crystal length decreased from 0.6cm to 0.1cm, an 83.3% reduction. *Momordica charantia* was the most sensitive, with a drastic drop to 0.6cm at 25% (42.9% reduction) and reaching 0.3cm at 100% (33.3% reduction). Overall, this extract achieved a total reduction of 0.75cm (71.4%), the highest among the three seed extract. Table.6 gives the cross-extract comparison of calcium urate crystal

Table. 6 Cross extract comparison

Parameter	<i>Cucumis sativus</i> (Seed)	<i>Cucurbita pepo</i> (Seed)	<i>Momordica charantia</i> (Seed)
Average length (0%)	1.05cm	1.05cm	1.05cm
Final average length (100%)	0.5cm	0.4cm	0.3cm
Maximum Reduction %	52.38%	61.9%	71.43%

3.3.3 Mass of Calcium urate crystals under the influence of the extracts

Table.7a Mass of the harvested calcium urate crystal under the influence of *Cucumis sativus* (seed), *Cucurbita pepo* (seed) and *Momordica charantia* (seed) extracts at various concentration of (0%, 25%, 50%,75% and 100%)

Concentration of the Extract	Name of the Extract / Mass of the Crystal (g)		
	<i>Cucumis sativus</i> (seed)	<i>Cucurbita pepo</i> (seed)	<i>Momordica charantia</i> (seed)
0%	0.59	0.59	0.59
25%	0.43	0.49	0.46
50%	0.31	0.25	0.29
75%	0.21	0.19	0.15
100%	0.19	0.14	0.08



Table.7a Mass of the harvested Calcium urate crystal under the influence of *Cucumis sativus* (seed), *Cucurbita pepo* (seed) and *Momordica charantia* (seed) extracts at various concentration of (0%, 25%, 50%,75% and 100%), Table. 7b gives Reduction% of average length of the Calcium urate crystal under the influence of *Cucumis sativus* (seed), *Cucurbita pepo* (seed) and *Momordica charantia* (seed) extract and Fig.12 shows the Bar diagram of length of the harvest Calcium urate crystal under the influence of *Cucumis sativus* (seed), *Cucurbita pepo* (seed) and *Momordica charantia* (seed) extracts at various concentration of (0%, 25%, 50%,75% and 100%)

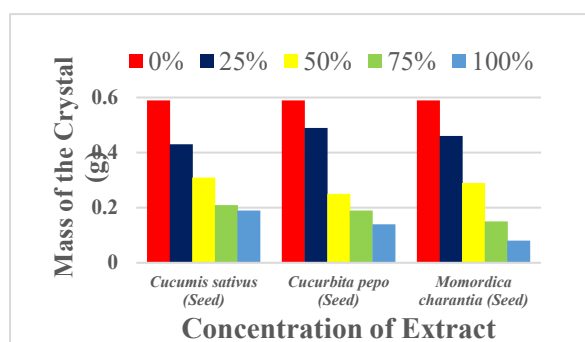


Fig.10 Bar diagram of length of the harvest Calcium urate crystal under the influence of *Cucumis sativus* (seed), *Cucurbita pepo* (seed) and *Momordica charantia* (seed) extracts at various concentration of (0%, 25%, 50%,75% and 100%)

Table. 7b Reduction% of average length of the Calcium urate crystal under the influence of *Cucumis sativus* (seed), *Cucurbita pepo* (seed) and *Momordica charantia* (seed) extract

Concentration	<i>Cucumis sativus</i> (CAUCS)		<i>Cucurbita pepo</i> (seed)-CAUCP		<i>Momordica charantia</i> (Seed) - CAUMC	
	Mass (g)	Reduction (%)	Mass (g)	Reduction (%)	Mass (g)	Reduction %
0%	0.59		0.59		0.59	
↓ 25%	0.43	0.16g (27.1%)	0.49	0.10 g (16.9%)	0.46	0.13 g (22.0%)
↓ 50%	0.31	0.12g (27.9%)	0.25	0.24 g (49.0%)	0.29	0.17 g (37.0%)
↓ 75%	0.21	0.10g (32.3%)	0.19	0.06 g (24.0%)	0.15	0.14 g (48.3%)
↓ 100%	0.19	0.02g (9.5%)	0.14	0.05 g (26.3%)	0.08	0.07 g (46.7%)

Cucumis sativus (cucumber) extract reduced calcium urate crystals significantly. At a 25% concentration, the crystals dropped from 0.59g to 0.43g, a reduction of 27.1%. Increasing the concentration to 50% lowered the mass further to 0.31g, which is a 27.9% reduction, making a total reduction of 47.5%. When the concentration increased to 75%, the mass decreased to 0.21g, a reduction of 32.3%, bringing the total reduction to 64.4%. Finally, at 100%, the mass fell to 0.19g, a small decrease of 9.5%. Overall, cucumber extract reduced the crystal mass by 0.40g, or 67.8%. *Cucurbita pepo* (pumpkin) extract also reduced the crystal mass. At 25%, it dropped from 0.59g to 0.49g, a 16.9% reduction.

When the concentration increased to 50%, the mass decreased to 0.25g, a reduction of 49%, resulting in a total reduction of 57.6%. At 75%, it dropped to 0.19g, a reduction of 24%, and at 100%, it fell to 0.14g, a 26.3% reduction. In total, pumpkin extract reduced the crystal mass by 0.45g, or 76.3%. *Momordica charantia* (bitter melon) extract showed the highest effect. At 25%, the crystals went from 0.59g to 0.46g, a 22% reduction. Increasing to 50% led to a decrease to 0.29g, a reduction of 37.5%, for a total reduction of 50.8%. At 75%, the mass fell to 0.15g, a reduction of 48.3%, and at 100%, it decreased to 0.08g, a 46.7% reduction. Overall, bitter melon extract reduced the crystal mass by 0.51g, or 86.4%, and Table 10 give the cumulative mass reduction % across all the extract.

Table .8 cumulative mass reduction % across all the extracts

Seed Extract	Final Mass (g)	Total Mass Reduced (g)	% Total Reduction
<i>Cucumis sativus</i>	0.24	0.44	64.7%
<i>Cucurbita pepo</i>	0.25	0.43	63.2%
<i>Momordica charantia</i>	0.14	0.54	79.4%

4. Conclusion

This study provides a detailed physicochemical and biological characterization of uric acid (UA) and calcium urate (CaU) crystals, along with a systematic evaluation of the anti-uricolytic potential of three plant seed extracts, namely *Cucumis sativus*, *Cucurbita pepo*, and *Momordica charantia*, against both crystal types. All three plant seed extracts progressively disrupted the characteristic crystal structure of both UA and CaU in a concentration-dependent manner. Higher concentrations transformed large, well-formed crystals into fine, fragmented particles. Quantitative inhibition studies demonstrated that all extracts significantly reduced the length of UA crystals over a 21-day period. *Cucumis sativus* showed



the most substantial early-stage inhibition (a 53.33% reduction at 25% concentration), while *Momordica charantia* achieved the highest cumulative length reduction of 80% at maximum concentration, comparable to *Cucumis sativus* and exceeding *Cucurbita pepo* (73.33%). Crystal dissolution assays supported these findings. *Momordica charantia* demonstrated the highest uricolytic efficacy against UA crystals, achieving a 79.4% total mass reduction, with a significant surge at maximum concentration due to the mobilization of bioactive constituents such as momordicin, charantin, alkaloids, and flavonoids. *Cucumis sativus* showed strong dissolution kinetics, with a cumulative reduction of 64.7%, while *Cucurbita pepo* displayed a gradual biphasic dissolution profile (63.2% cumulative reduction). Against CaU crystals, *Momordica charantia* again recorded the highest dissolution rate (86.4% mass reduction), followed by *Cucurbita pepo* (76.3%) and *Cucumis sativus* (67.8%). Thus, these findings indicate that the seed extracts of *Cucumis sativus*, *Cucurbita pepo*, and *Momordica charantia* have significant anti-urolithic activity through complementary mechanisms of crystal growth inhibition and dissolution. *Momordica charantia* (seed) emerged as the most potent candidate across both crystal models, thanks to its unique concentration-dependent kinetics and rich phytochemical composition. These results provide a strong scientific basis for developing plant-derived therapeutic strategies for managing uric acid nephrolithiasis and hyperuricemia-associated disorders. Future research using in vivo models and isolating specific bioactive fractions is necessary to further explore the molecular mechanisms underlying these anti-urolithic effects.

Reference

- [1]. Dalbeth, N., Merriman, T. R., & Stamp, L. K. (2016). Gout. *The Lancet*, 388(10055), 2039–2052. [https://doi.org/10.1016/S0140-6736\(16\)00346-9](https://doi.org/10.1016/S0140-6736(16)00346-9)
- [2]. Borghi, C., Agabiti-Rosei, E., Johnson, R. J., et al. (2020). Hyperuricaemia and gout in cardiovascular, metabolic and kidney disease. *European Journal of Internal Medicine*, 80, 1–11. <https://doi.org/10.1016/j.ejim.2020.07.006>
- [3]. Kuo, C. F., Grainge, M. J., Zhang, W., & Doherty, M. (2015). Global epidemiology of gout: Prevalence, incidence and risk factors. *Nature Reviews Rheumatology*, 11(11), 649–662. <https://doi.org/10.1038/nrrheum.2015.91>
- [4]. Sharma, S.D.R., Selvaraju, R. Structural, thermal and electrochemical analysis of in vitro grown urinary stone type uric acid crystal. *Discov. Chem.* 3, 32 (2026). <https://doi.org/10.1007/s44371-026-00479-x>
- [5]. Khan SR, Byer KJ, Thamilselvan S, et al. Crystal-cell interaction and apoptosis in oxalate-associated injury of renal epithelial cells. *Journal of the American Society of Nephrology : JASN*. 1999 Nov;10 Suppl 14:S457-63. PMID: 10541283.
- [6]. Grammer, A. C., & Lipsky, P. E. (2017). Drug repositioning strategies for the identification of novel therapies for rheumatic autoimmune inflammatory diseases. *Rheumatic diseases clinics of North America*, 43(3), 467-480. <https://doi.org/10.1016/j.rdc.2017.04.010>.
- [7]. Menon, S., Al-Saadi, A. S., Al-Aamri, N. J., Al-Jaradi, A. Z. H., Al Mamari, H. K., Al Haddabi, L. H., & Shinisha, C. B. (2022). Inhibition of crystallization of calcium oxalate monohydrate using leaves from different species of Moringa—Experimental and theoretical studies. *Journal of Crystal Growth*, 598, 126859. <https://doi.org/10.1016/j.jcrysgro.2022.126859>.
- [8]. Al-Dhafri, K. S., Farooq, S. A., Eltayeb, E., & Bahry, S. N. (2014). Antimicrobial compounds from ethanomedicinal plants of Oman. In *Biotechnology and Conservation of Species from Arid Regions* (pp. 311-326). Nova Science Publishers, Inc..
- [9]. Javid, Hina & Fatima, Urooj & Rukhsar, Aqsa & Hussain, Shabbir & Bibi, Shagufta & Bodlah, Muhammad & Shahzad, Hafiza & Dilshad, Muhammad & Waqas, Muhammad & Sharif, Ayesha. (2024). Phytochemical, Nutritional and Medicinal Profile of *Cucumis sativus* L. (Cucumber). *Food Science and Engineering*. 358-377. 10.37256/fse.5220244795.
- [10]. Iu, Karaye & Fardami, Aminu & Ny, Garba & Hm, Lawal. (2025). Nutritional and Phytochemical Profiling of the Fruit Pulp and Seeds of Cucumber (*Cucumis sativus* L.): Implication for Dietary Health in Sokoto- Nigeria. *International Journal of Advanced Multidisciplinary Research and Studies*. 5. 1374-1379. 10.62225/2583049X.2025.5.3.4459.
- [11]. Theil G, Richter M, Schulze M, Köttig T, Patz B, Heim S, Krauß Y, Markov M, Fornara P. Extract from *Cucurbita pepo* improves BPH symptoms without affecting sexual function: a 24-month noninterventional study. *World J Urol*. 2022 Jul;40(7):1769-1775. doi: 10.1007/s00345-022-04036-w. Epub 2022 May 27. Erratum in: *World J Urol*. 2022 Oct;40(10):2589-2590. doi: 10.1007/s00345-022-04132-x. PMID: 35622117; PMCID: PMC9236993.
- [12]. Kubola J, Siriamornpun S. Phenolic contents and antioxidant activities of bitter gourd (*Momordica charantia* L.) leaf, stem and fruit fraction extracts in vitro. *Food Chem*. 2008 Oct 15;110(4):881-90. doi:



- 10.1016/j.foodchem.2008.02.076. Epub 2008 Mar 4. PMID: 26047274.
- [13].Trojanowicz, M. (2020). Flow Chemistry in Contemporary Chemical Sciences: A Real Variety of Its Applications. *Molecules*, 25(6), 1434. <https://doi.org/10.3390/molecules25061434>.
- [14].Murugaiyah V, Chan KL. Mechanisms of antihyperuricemic effect of Phyllanthus niruri and its lignan constituents. *J Ethnopharmacol.* 2009 Jul 15;124(2):233-9. doi: 10.1016/j.jep.2009.04.026. Epub 2009 May 3. PMID: 19397979.
- [15].Shi, Y., Evans, J. & Rock, K. Molecular identification of a danger signal that alerts the immune system to dying cells. *Nature* 425, 516–521 (2003). <https://doi.org/10.1038/nature01991>.
- [16].Joseph B, Jini D. Antidiabetic effects of *Momordica charantia* (bitter melon) and its medicinal potency. *Asian Pac J Trop Dis.* 2013 Apr;3(2):93–102. doi: 10.1016/S2222-1808(13)60052-3. PMID: 24027280.
- [17].Liu Z, Gong J, Huang W, Lu F, Dong H. The Effect of *Momordica charantia* in the Treatment of Diabetes Mellitus: A Review. *Evid Based Complement Alternat Med.* 2021 Jan 16;2021:3796265. doi: 10.1155/2021/3796265. PMID: 33510802; PMCID: PMC7826218.
- [18].Mahwish, Saeed F, Sultan MT, Riaz A, Ahmed S, Bigiu N, Amarowicz R, Manea R. Bitter Melon (*Momordica charantia* L.) Fruit Bioactives Charantin and Vicine Potential for Diabetes Prophylaxis and Treatment. *Plants (Basel).* 2021 Apr 8;10(4):730. doi: 10.3390/plants10040730. PMID: 33918062; PMCID: PMC8070166.
- [19].Jia S, Shen M, Zhang F, Xie J. Recent Advances in *Momordica charantia*: Functional Components and Biological Activities. *Int J Mol Sci.* 2017 Nov 28;18(12):2555. doi: 10.3390/ijms18122555. PMID: 29182587; PMCID: PMC5751158.
- [20].Beghalia, Mohamed & Said, Ghalem & Allali, Hocine & Belouatek, Aissa & Marouf, Abderrazak. (2008). Inhibition of calcium oxalate monohydrate crystal growth using Algerian medicinal plants. *Journal of Medicinal Plants Research.* 2. 66-70.
- [21].Vijayaprasath, R., Selvaraju, R., & Renuka Devi, K. B. (2025). Spectroscopical Investigation of Human Grown Urinary Calculi in and Around Puducherry Region. *International Journal of Scientific Research in Science, Engineering and Technology*, 12(4), 84-97.
- [22].Sakuntala, P., Ch. Pradyutha, A., & Selvaraju, R. (2024). Analysis of minerals and phytochemicals in the leaves of the *Ocimum kilimandscharicum* plant using spectroscopic methods and screening of antibacterial activity. *Natural Product Research*, 1-7.
- [23].Selvaraju, R., & Bhuvanewari, M. (2020). Growth and Spectral Investigation on Pure Calcium Phosphate Doped With (Copper and Magnesium) Crystals.
- [24].Selvaraju R, Alli J, Sulochana S, & Bhuwanewari M. (2017). Dissolution studies in few urinary type crystals. *JOURNAL OF ADVANCED APPLIED SCIENTIFIC RESEARCH*, 1(7). <https://doi.org/10.46947/joaasr17201741>
- [25].Krishnaveni, T., Valliappan, R., Selvaraju, R., & Prasad, P. N. (2016). Preliminary phytochemical, physicochemical and antimicrobial studies of *Loranthus elasticus* of Loranthaceae family. *Journal of Pharmacognosy and Phytochemistry*, 5(6), 7.
- [26].Shatri, A. M. (2021). Ethnomedicinal uses, phytochemical characterization, and antibacterial activity of *Grewia tenax* and *Albizia anthelmintica* extracts against multidrug-resistant pneumonia-causing bacteria.
- [27].Bollona, J. P. B., Paredes, G. E. D., Wagner, M., & Idrogo, C. R. (2019). In vitro tissue culture, preliminary phytochemical analysis, and antibacterial activity of *Psittacanthus linearis* (Killip) JK Macbride (Loranthaceae). *Revista Colombiana de Biotecnología*, 21(2), 22-35.
- [28].Selvaraju, R., & Sulochana, S. (2016). In-vitro growth and inhibition studies of *Tribulus terrestris* on calcium oxalate monohydrate crystals. *International Journal of Science and Research*, 5(6), 83-87.
- [29].Selvaraju, R., Raja, A., & Thiruppathi, G. (2015). FT-IR spectroscopic, thermal analysis of human urinary stones and their characterization. *Spectrochimica Acta Part A: Molecular and Biomolecular Spectroscopy*, 137, 1397-1402. <https://doi.org/10.1016/j.saa.2014.09.04>.
- [30].Vasuki, G., & Selvaraju, R. (2014). Growth and characterization of uric acid crystals. *International Journal of Science and Research*, 3(8), 696-699.